Original Article

Enhanced Joint Heart and Respiratory Rates Extraction from Functional Near-infrared Spectroscopy Signals Using Cumulative Curve Fitting Approximation

Navid Adib, Seyed Kamaledin Setarehdan, Shirin Ashtari Tondashti, Mahdis Yaghoubi

Department of Engineering, School of Electrical and Computer Engineering, University of Tehran, Tehran, Iran

Abstract

Background: Functional near-infrared spectroscopy (fNIRS) is a valuable neuroimaging tool that captures cerebral hemodynamic during various brain tasks. However, fNIRS data usually suffer physiological artifacts. As a matter of fact, these physiological artifacts are rich in valuable physiological information. **Methods:** Leveraging this, our study presents a novel algorithm for extracting heart and respiratory rates (RRs) from fNIRS signals using a nonstationary, nonlinear filtering approach called cumulative curve fitting approximation. To enhance the accuracy of heart peak localization, a novel real-time method based on polynomial fitting was implemented, addressing the limitations of the 10 Hz temporal resolution in fNIRS. Simultaneous recordings of fNIRS, electrocardiogram (ECG), and respiration using a chest band strain gauge sensor were obtained from 15 subjects during a respiration task. Two-thirds of the subjects' data were used for the training procedure, employing a 5-fold cross-validation approach, while the remaining subjects were completely unseen and reserved for final testing. **Results:** The results demonstrated a strong correlation ($r > 0.92$, Bland–Altman Ratio <6%) between heart rate variability derived from fNIRS and ECG signals. Moreover, the low mean absolute error (0.18 s) in estimating the respiration period emphasizes the feasibility of the proposed method for RR estimation from fNIRS data. In addition, paired *t*-tests showed no significant difference between respiration rates estimated from the fNIRS-based measurements and those from the respiration sensor for each subject ($P > 0.05$). **Conclusion:** This study highlights fNIRS as a powerful tool for noninvasive extraction of heart and RRs alongside brain signals. The findings pave the way for developing lightweight, cost-effective wearable devices that can simultaneously monitor hemodynamic, heart, and respiratory activity, enhancing comfort and portability for health monitoring applications.

Keywords: *Functional near-infrared spectroscopy, cumulative curve fitting approximation, heart rate variability, respiratory rate*

Submitted: 27-Jul-2024 **Revised:** 14-Oct-2024 **Accepted:** 02-Nov-2024 **Published:** 01-May-2025

Introduction

Functional near-infrared spectroscopy (fNIRS) has emerged as a valuable tool for examining changes in cerebral hemodynamics and oxygen saturation levels both during specific brain tasks and at rest.[1] Over the past 30 years, fNIRS has provided insights into the hemodynamic reactions associated with cognitive, visual, and motor activities, while also evaluating brain functional connectivity.[2-4] NIRS measurements rely on detecting red and near-infrared light as it traverses through perfused tissue. This light is administered through the skin, and the scattered light is gathered at a specified distance from the emitting source. The separation between the emitter and collector (or detector) dictates the route taken by the collected light. For the light to penetrate the cerebral vasculature effectively, the distance between the emitter and collector should exceed 2.5 cm in adults.[5] In comparison to other neuroimaging techniques such as electroencephalography (EEG) and functional magnetic resonance imaging (fMRI), fNIRS offers superior spatial and temporal resolutions, respectively.[6] Consequently, fNIRS has

How to cite this article: Adib N, Setarehdan SK, Tondashti SA, Yaghoubi M. Enhanced joint heart and respiratory rates extraction from functional near-infrared spectroscopy signals using cumulative curve fitting approximation. J Med Signals Sens 2025;15:15.

Address for correspondence:
Dr. Seyed Kamaledin Setarehdan,
North Kargar St., Tehran 1439957131, Iran.
E-mail: ksetareh@ut.ac.ir

Access this article online

Website: www.jmssjournal.net

DOI: 10.4103/jmss.jmss_48_24

Quick Response Code:

been widely utilized in a variety of studies spanning different cognitive tasks and clinical settings.[7]

The hemodynamic signal exhibits two types of artifacts: physiological artifacts such as heartbeat, Mayer[8] and respiration, and nonphysiological interferences such as motion artifacts[9] and electrical noises. Various algorithms, including wavelet analysis,[10] conventional[11] or adaptive filtering,[12] Kalman filtering,[13] independent component analysis[14] and deep learning,[15] are capable of attenuating physiological artifacts and other sources of noise. Among these, the artifacts originating from heartbeats and respiration can be extracted from fNIRS signals. These signals can then be effectively leveraged for heart rate (HR) and respiratory rate (RR) analysis, offering additional valuable insights. Consequently, utilizing a single portable device enables the extraction of three distinct signals containing crucial functional information from the brain, heart, and respiration.

HR variability (HRV) parameters quantify the variation in time intervals between successive cardiac cycles. This metric has been established as a valuable tool for characterizing and comprehending the regulation of the cardiovascular system by the autonomic nervous system (ANS).[16] The gold standard for HR tracking, involves analyzing the interbeat intervals (IBIs) identified through an electrocardiogram (ECG) signal.[17] Numerous studies have aimed to measure HR and HRV using fNIRS signals. For instance, Hakimi and Setarehdan[18] employed a band pass filter to isolate the heart signal from fNIRS data and utilized peak detection algorithms for real-time extraction of IBIs and HRV.

Respiration serves as the largest oscillator in the body, intricately involved in regulating physiological processes in response to environmental demands and ensuring the maintenance of homeostasis.[19] Respiratory activation serves as an indicator not only of metabolic alterations but also of psychological and behavioral processes.[20] Research on extracting RR from fNIRS signals remains relatively sparse, with the predominant apparatus used for RR extraction being respiratory inductive plethysmography, strain gauge, and spirometry. However, in a recent study, Hakimi *et al*.[21] introduced novel techniques to extract respiration rate from fNIRS data. They utilized a band pass filter (0.05 Hz to 2 Hz) to isolate the respiratory signal and extracted baseline wander from troughs of the filtered signal. The peak of the frequency spectrum was then used to determine RR. This approach represents a promising advancement in the field, offering new insights into respiratory dynamics through fNIRS technology.

In fNIRS signals, noticeable drifts are frequently observed.[22] Wide sense stationarity requires the first two statistical moments to remain constant over time. Consequently, signals exhibiting drift are automatically categorized as nonstationary. In addition, components stemming from neuronal hemodynamic responses demonstrate a time-varying second statistical moment. Various tools such as bandpass filtering (BPF), LPF,[23] and DCT[24] have traditionally been utilized for extracting the hemodynamic response signal. However, recent advancements by Patashov *et al*.[22,25] introduced and applied cumulative curve fitting approximation (CCFA), a nonstationary and nonlinear filter. This filter helps mitigate distortion effects arising from the nonstationarity of fNIRS data. While previous studies have utilized CCFA for extracting the hemodynamic response signal with favorable outcomes, its application for filtering fNIRS signals to extract physiological artifacts such as HR and respiration-related signals has not been explored before.

Estimating joint heart and RRs, as well as extracting HRV from fNIRS signals, is crucial for advancing comprehensive physiological monitoring. The simultaneous assessment of cerebral activity, HR, and respiration using a single sensor enables perfectly time-synchronized evaluations of (cerebral) physiology, providing a more holistic understanding of the body's responses.[26] Furthermore, research has demonstrated that incorporating cardiac and respiratory features extracted from fNIRS data can enhance the accuracy of mental workload classification, illustrating the broader potential of fNIRS for multiparameter monitoring.[27] However, the extraction of HR and respiration-related signals from fNIRS has been underexplored, particularly in addressing nonstationarity. To fill this gap, we aimed to assess the effectiveness of the CCFA technique in extracting heart and RRs from fNIRS signals, providing a novel approach to handle the inherent drift and distortion in the data. It is hoped that the results of this research will aid in the creation of a device with lower power consumption, reduced weight, volume, and cost, making it both efficient and highly suitable for use in portable and wearable physiological monitoring systems.

Materials and Methods

Participants

The experiments in this study have an ethics code of IR.UT.SPORT.REC.1402.102 from the research ethics committees of the University of Tehran, faculty of sport sciences and health. Data acquisition includes concurrent recordings of fNIRS, ECG, and respiratory signals were obtained from a group of 15 healthy adult males and females with an average age of 27 (±3.1) years. Before participation, participants self-reported no history of heart, respiratory, or neurological diseases, and confirmed that they were not taking any medication that could affect the outcomes of the study. All participants were fully informed about the experiment and provided written consent before the commencement of the study. Data from two-thirds of the subjects were utilized for training and parameter tuning through a 5-fold cross-validation process, while the data from the remaining five subjects remained unseen

throughout the entire procedure and were designated as the test dataset for evaluating the final results.

Data acquisition protocol

In this study, the Oxymap124 fNIRS system of the NIR laboratory of the University of Tehran was employed for data acquisition.[28] This system uses light sources emitting at wavelengths of 730 nm and 850 nm. A sampling rate of 10 Hz was set for data recording. Only one fNIRS channel positioned at the midline (Fpz) on the 10–20 system with an inter source-detector distance of 25 mm was utilized [Figure 1a]. The ECG signal from standard lead I was recorded simultaneously using three electrodes positioned at the sites right arm, left arm, and right leg [Figure 1b], utilizing the AD8232 biopotential sensor. The sampling rate for the ECG signals was set to 660 Hz, which is more than sufficient to capture the primary frequency range of ECG (0.5–40 Hz), ensuring precise detection of HRV and other cardiac features. Respiratory signals were concurrently recorded using a chest-band strain gauge at a sampling rate of 6.6 Hz, which is adequate for capturing the slower frequency components of respiration (typically between 0.1 Hz and 0.5 Hz). For every 100 samples of ECG, 1 sample of respiration was collected, ensuring synchronized data acquisition with appropriate resolution for both signals.

Task

Before commencing the experiment, participants were provided with a detailed briefing regarding the experimental procedure. They were instructed on how to perform the tasks involved in the study, ensuring that they understood the requirements and protocols to be followed. The data recording protocol for RR estimation, adapted from references[21,29] is depicted in Figure 2. The protocol comprised one block of a resting period lasting for 60 s (A), succeeded by two blocks of breathing control tasks (B and D), with a 30 s rest period in between (C). Following this, the same sequence of blocks was repeated. The participants were instructed to maintain a steady pace of inhalation and exhalation at specified rates while observing a vertical (bar chart as a graphical shape) moving synchronously with text indicating the respective inhale and exhale phases displayed on the screen. Each block of the breathing control task comprised 5 steps, with a consistent respiration rate maintained over a duration of 50 s. In general, respiration was performed at intervals of 3.5, 4.75, 6, 7.25, and 8.5 s, each repeated four times.

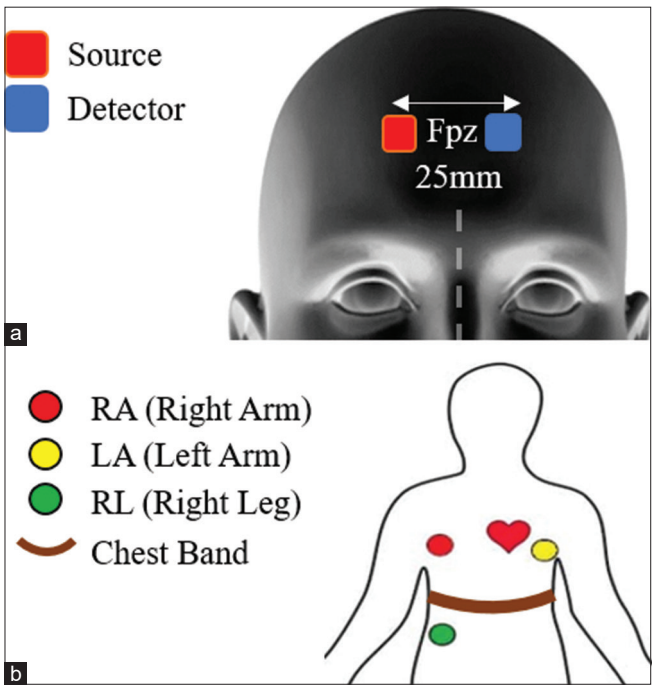

Figure 1: Electrode placement for physiological measurements. (a) Functional near-infrared spectroscopy source-detector locations, (b) Placement of electrocardiogram electrodes and respiration sensors

Processing

Cumulative curve fitting approximation

In this work, the CCFA technique is used for signal processing. CCFA utilizes a sliding window of k_{ord} size, incorporating k_{ord} points to fit curves to the input signal. The resulting filtered output is derived from the average extension of these curves at designated points. The reconstructed signal, denoted as $Sig(n)$, is obtained using Eq. 1.[22]

$$Sig(n)=\frac{P_{n-k_{ord}+1}(k_{ord}-1)+P_{n-k_{ord}+2}(k_{ord}-2)+\ldots+P_n(0)}{k_{ord}} \quad (1)$$

Here, $n = 1, 2,..., L$ denotes the index of the sample being corrected. In addition, $P_q(j)$ denotes the polynomial curve fitting function calculated using the samples within a window size of length k_{ord} (i. e.,$[q - k_{ord} +1, q - k_{ord} +2,..., q]$).

To further clarify, in this equation, $P_{n-k_{ord}+1}(k_{ord}-1)$ refers to a polynomial fitted using samples from $[n-2k_{ord}+2 : n-k_{ord}+1]$. This polynomial is then extrapolated up to $k_{ord}-1$ points, specifically at the location of sample n, and its value is then used in the equation. In addition, in Eq. 1, other polynomials are computed based on their respective windows of samples, and each polynomial $P_{ord}=1$ is similarly extended until it precisely reaches the position of sample n, where their values are incorporated into the equation. For this process, a linear, first-degree polynomial is employed as the curve fitting function. An illustration showcasing the computation of CCFA for time $n=6$, utilizing $_{ord}=3$ and a linear polynomial function for fitting, is presented in Figure 3.

Functional near-infrared spectroscopy filtering procedure

The main processing diagram, depicted in Figure 4, outlines the signal processing steps. Initially, the optical signal obtained at 850 nm as a time signal x (t), is subjected for processing using the CCFA method with a window

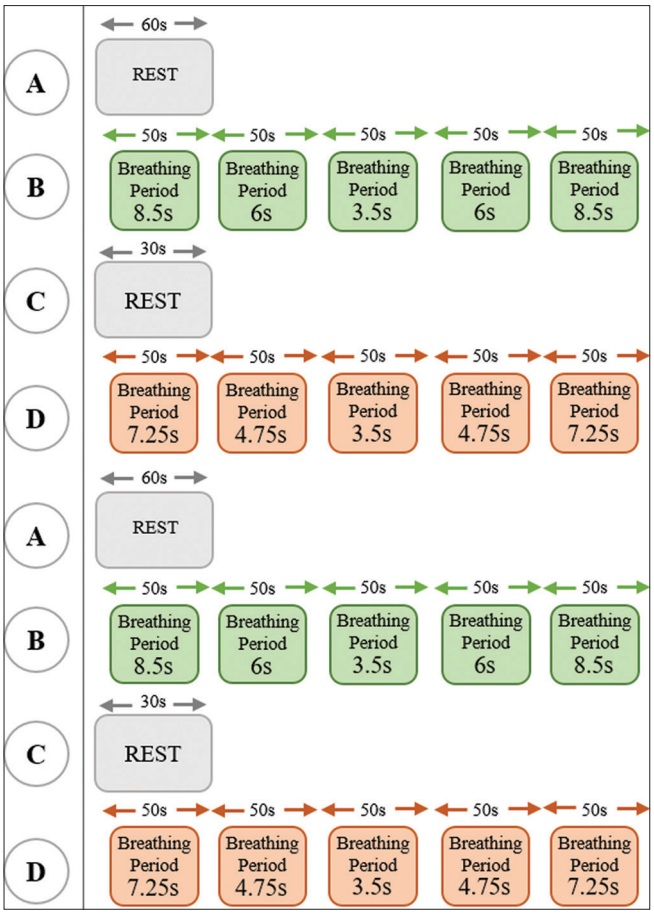

Figure 2: The breathing task protocol. It consists of a 60-s resting period (A) followed by two 250-s breathing control tasks (B, D), separated by a 30-s rest (C). The same blocks were repeated again

size of 2.5 s. The selection of the 850 nm wavelength over 730 nm was motivated by its sensitivity to fluctuations in heart activity and superior signal-to-noise ratio. This processing step effectively removes higher-order frequency contamination, resulting in $z_1(t)$, which primarily contains information related to drift and respiration, while the heart component is not present. Simultaneously, the raw fNIRS signal undergoes separate processing using CCFA with a larger window size of 7 s. This processing step aims to cancel out the respiratory component and higher frequency contaminations, leaving information primarily associated with drift and brain-related activity, obtained as $z_2(t)$. Subsequently, the heart component is isolated by subtracting x (t) from $z_1(t)$. This subtraction obtained as $y_1(t)$, isolates the heart-related signals, which are then suitable for further analysis using peak detection algorithms to derive HR and HRV metrics. In addition, the respiratory component is isolated by subtracting $z_1(t)$ from $z_2(t)$. This subtraction obtained as $y_2(t)$, results in the extraction of signals specifically related to respiration, which are then ready for further analysis to extract respiration rate information.

The FFT of $y_1(t)$ and $y_2(t)$ is also displayed in Figure 4. It illustrates that in $y_1(t)$, the frequency component of the

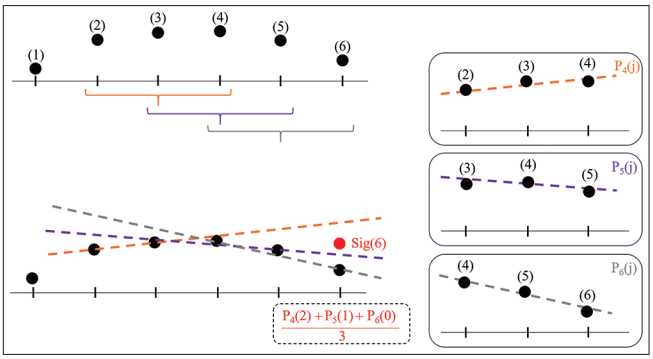

Figure 3: Illustration of cumulative curve fitting approximation calculation for time *n* = 6 with k_ord = 3

heart-related signal is extracted, while other frequencies are cancelled out. Similarly, in $y_2(t)$, the FFT demonstrates that the respiration component is extracted, while other frequencies such as the heart signal or lower frequencies like drift are effectively cancelled.

The initial 10 s of $y_1(t)$, encompassing heart-related components, were employed for signal quality assessment. Similar to the methodology described in article,[30] the scalp coupling index (SCI) is computed. Favorable skin contact between the optodes and the scalp usually leads to a noticeable variation correlating with cardiac pulsation, which predominates in the raw data.[31] The SCI for each subject's single channel is determined as the correlation between the signals of the two wavelengths. Channels deemed to have poor signal quality were excluded based on the SCI assessment.

Peak detection

In the next step, it is necessary to accurately localize the peaks related to the heart and respiration signals from $y_1(t)$ and $y_2(t)$, respectively. To achieve this, a simple window-based technique is employed, wherein a peak is detected if the middle point of the window exhibits a maximum value compared to its surrounding points. The selection of the window size is crucial and is determined based on the sampling frequency and the nature of the target signal (heart or respiration). This careful selection helps prevent the detection of erroneous local maxima and ensures that correct maximum peaks are not missed. Given the limited temporal resolution of samples and peaks of the heart due to the 10 Hz sampling frequency of fNIRS, which corresponds to a temporal resolution of 0.1 s, alternative methods are employed to enhance precision. Although resampling techniques such as those utilized in article,[32,33] which employed the RESAMPLE function of MATLAB to up-sample data from 10 Hz to 100 Hz, could be considered, new real-time algorithm for correcting peak locations, based on polynomial fitting, is applied. In this method, a second-order polynomial function is fitted for each detected peak, spanning across the detected peak and its adjacent left and right samples. Subsequently, the maximum of this polynomial function is computed and considered as the final peak, thus ensuring

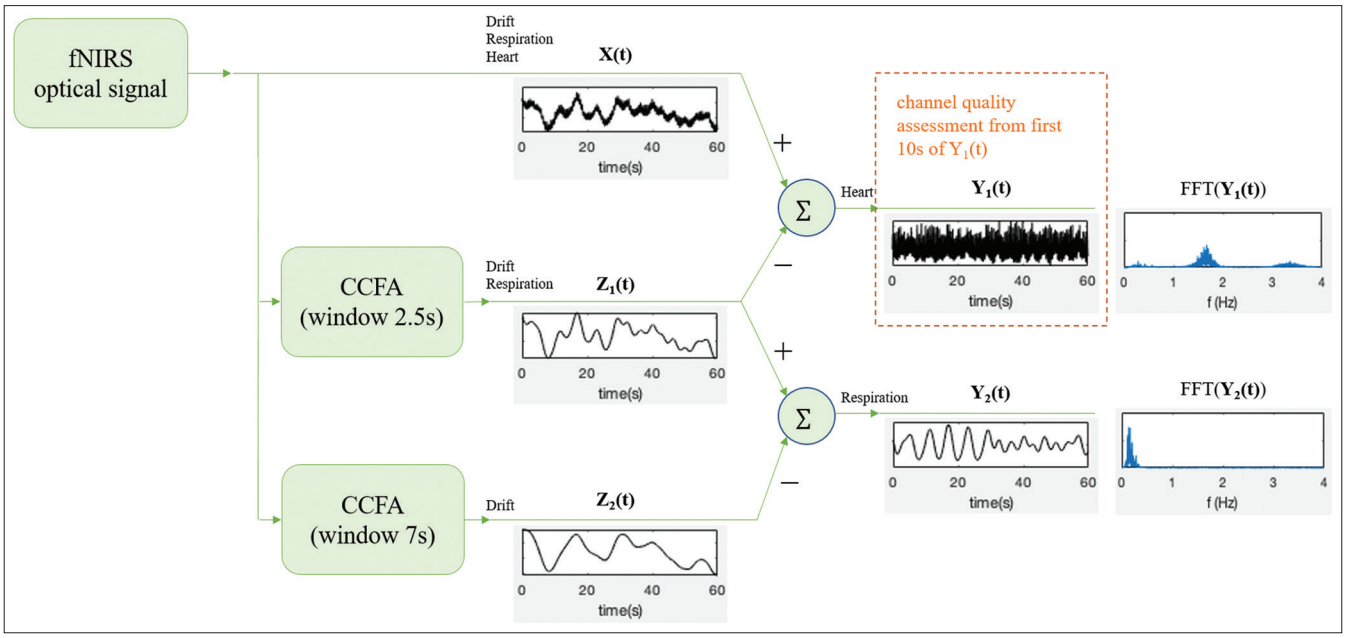

Figure 4: The main block diagram of proposed method. fNIRS: Functional near-infrared spectroscopy, CCFA: Cumulative curve fitting approximation

improved accuracy in peak localization despite the limitations in temporal resolution. The main steps of peak detection are summarized in Algorithm 1 as follows:

Algorithm 1: Localization of filtered fNIRS signal peaks

Input: filtered optical intensity 850 nm signal x(n) and time t(n), Window size 2N+1
Output: time of each peaks J

```
J ← []
for i = N+1 to Length(x(n)) -N do
  % window is N neighbors left and N neighbors right of x(i)
  window ← [x(i-N:i-1); x(i+1:i+N)]
  % new peak is detected
  if x(i) > max(window) then
    A ← [t(i-1) ^2, t(i-1), 1; t(i)^2, t(i), 1; t(i+1) ^2, t(i+1),1]
    B ← [x(i-1); x(i); x(i+1)]
    % find a, b, c in [ax^2 + bx + c].
    % in Matlab A\B performs matrix left division solving the equation A * X = B for X
    X ← A\B;
    location of peak ← -1* X(2) / (2* X(1)); % -b/2a is location of peak
    J ← [J location of peak] % add it to list
  end if
end for
return J
```

After the extraction of the heart beat and respiration signals, both HR and RR are measured by calculating the time interval between two adjacent peaks in their respective signals. For HR, the time interval between successive peaks in the heart beat signal represents the IBI, which is used to determine HR in beats per minute (BPM). Similarly, for RR, the time interval between consecutive peaks in the respiration signal represents the respiration period, which is used to determine RR in breaths per minute (BPM). By quantifying these time intervals, HR and RR can be accurately assessed, providing essential physiological information for various applications in health care and research. In addition to HR and RR, HRV is also calculated. HRV refers to the variation in the time interval between successive heartbeats and is an important indicator of ANS activity and cardiovascular health. The peak detection algorithm described in Algorithm 1 is utilized to identify peaks in both the respiration sensor data obtained from the strain gauge and the ECG signal. Before applying this algorithm to the respiration data, a smoothing process is performed using the SMOOTH function in MATLAB with a window length of 3s.

Results

Channel quality assessment

The SCI was computed for each single channel of all participants, and all channels were deemed acceptable as their SCI values exceeded the recommended threshold of 0.8.[31] Therefore, no data were excluded from further processing.

Optimizing cumulative curve fitting approximation window sizes

Considering the fact that CCFA had not been previously utilized for fNIRS data filtering in order to extract heart and respiration related components, determining the optimal window sizes for short and long wave-patterns is a challenging issue. To address this, A series of filtrations was conducted using various window sizes. Specifically, a range of window sizes from 1 to 3.5 s, with increments of 0.5 s, was explored on the training dataset, utilizing 5-fold cross-validation. By employing the power spectral density ratio (PSDR) as defined in Eq. 2, the objective was to identify a window size that effectively eliminated heart-related components while preserving those related to respiration. The goal was to minimize the PSDR of $z_1(t)$, indicating

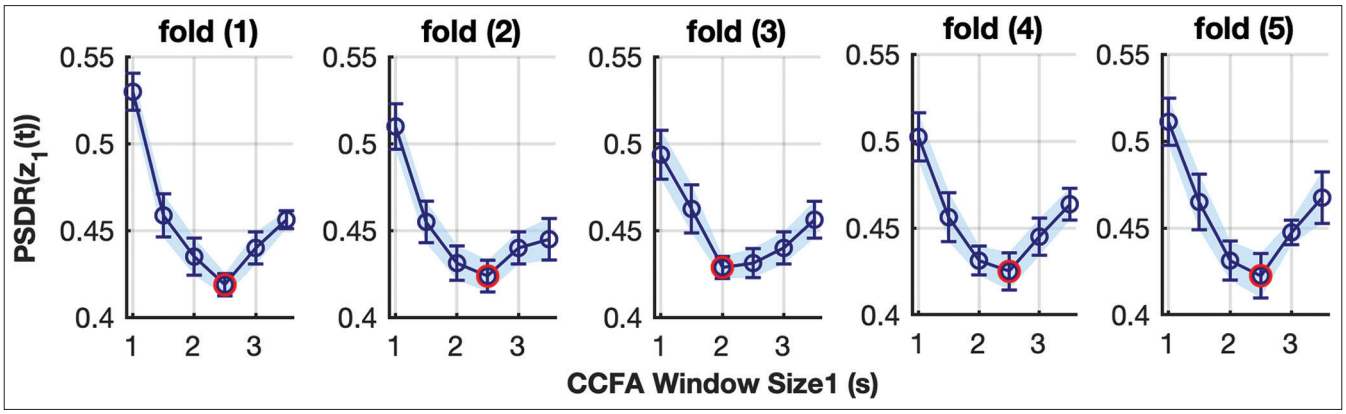

Figure 5: Tuning the initial (small) window size in the proposed method using the training dataset with 5-fold cross-validation. The power spectral density ratio criteria were evaluated for different cumulative curve fitting approximation (CCFA) window sizes ranging from 1 s to 3.5 s, with increments of 0.5 s. Rather than concentrating only on fold 3, results from the other folds suggest that a window size of 2.5 s is suitable for the CCFA. CCFA: Cumulative curve fitting approximation, PSDR: Power spectral density ratio

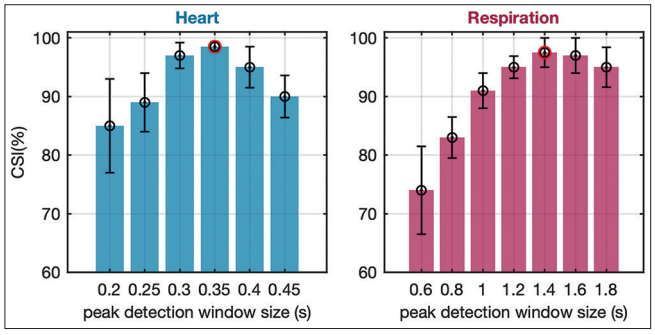

Figure 6: Critical success index criteria evaluated over different peak detection window sizes. For heartbeat detection, the window sizes were set between 0.2 and 0.45 s, with increments of 0.05 s, while for respiration detection, the window sizes ranged from 0.6 to 1.8 s, with increments of 0.2 s. The results from the training dataset show that the highest criteria were achieved at 0.35 s for heart detection and 1.4 s for respiration detection. CSI: Critical success index

successful removal of heart-related signals while retaining the respiration-related signals. As shown in Figure 5, results of the cross-validation indicate that the majority of cases achieved optimal performance with a window size of 2.5 s.

$$PSDR = \frac{\int_{1}^{2.5} PSD(z_1(t))}{\int_{0.1}^{0.5} PSD(z_1(t))} \quad (2)$$

Subsequently, having identified the appropriate window size for the initial CCFA (with a smaller window size), we proceeded to apply the next CCFA with a window size range of 4–9 s, employing a 1-s step. Here, the correlation of the output with the signal of respiration strain gauge sensor was utilized as a selection criterion. This comprehensive approach enabled us to systematically determine the optimal window sizes for CCFA filtration, ensuring robust extraction of heart and respiration related components from fNIRS data. At the end of this process, the optimum window size calculated on our train dataset was found to be 7 s.

Optimizing the peak detection window size

To refine the optimal window size for the peak detection algorithm, the training dataset is used. The critical success index defined in Eq. 3 was employed as the peak detection criterion,[21] resulting in the determination of the optimal window size (N). Here *TP*, *FN* and *FP* stand for correctly, missed and wrongly detected peaks. As indicated by the results in Figure 6 from the training dataset, the optimal window size for heartbeat detection was determined to be 0.35 s, whereas for respiration detection, it was found to be 1.4 s.

$$CSI = \frac{T_P}{T_P + F_N + F_P} \quad (3)$$

Result of applying respiratory rate estimation algorithm to *in vivo* measured functional near-infrared spectroscopy signal

Figure 7 (top) shows the fNIRS signal alongside the filtered fNIRS signal using a conventional Butterworth bandpass filter with cutoff frequencies of 1–1.9 Hz, similar to the method in article.[18] as well as the filtered fNIRS signal obtained using the proposed CCFA method, with their respective peaks. In addition, the ECG signal is displayed. The lower section presents the HRV derived from the proposed algorithm and conventional BPF, superimposed with the HRV signal derived from the ECG as the reference HRV.

To objectively assess the performance of the algorithms employed for HR derivation from the fNIRS signal, several quantitative metrics were calculated. These metrics include:

1. Mean error: The average difference between the HR derived from fNIRS (HR from fNIRS) and the reference HR obtained from ECG (HR from ECG)
2. Maximum error: The maximum absolute difference between HR from fNIRS and HR from ECG
3. Spearman linear correlation between HR from fNIRS and HR from ECG

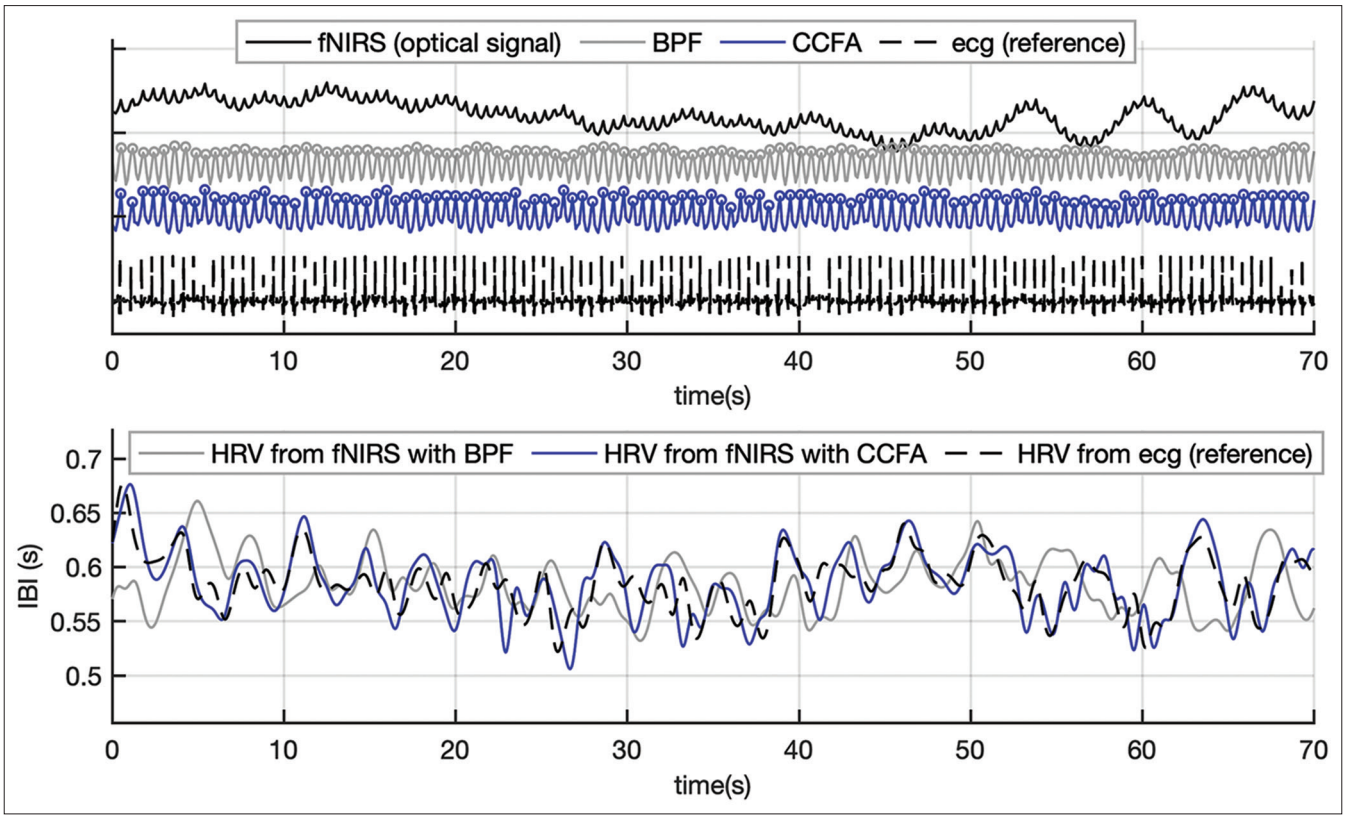

Figure 7: Comparison of heart rate variability (HRV) signals derived from functional near-infrared spectroscopy (fNIRS) and electrocardiogram (ECG) Top-Raw optical fNIRS signal, fNIRS filtered with bandpass filter (BPF), fNIRS processed with the proposed cumulative curve fitting approximation (CCFA) method, and reference ECG signal. Bottom-HRV signals derived from BPF, CCFA, and reference ECG. IBI: Inter beat interval, HRV: Heart rate variability, fNIRS: Functional near-infrared spectroscopy, BPF: Bandpass filter, CCFA: Cumulative curve fitting approximation

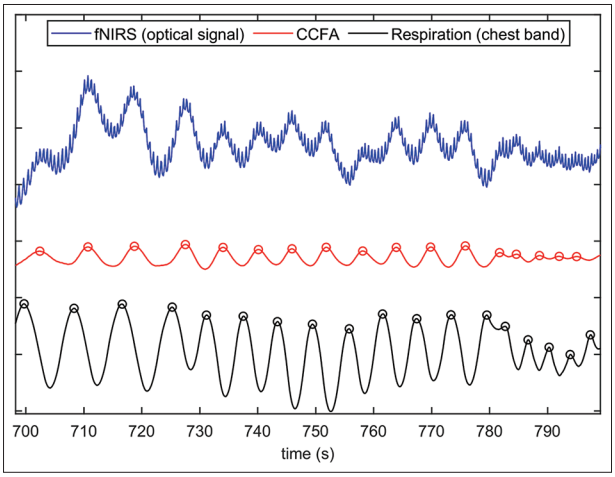

Figure 8: Comparison of functional near-infrared spectroscopy (fNIRS), filtered fNIRS with cumulative curve fitting approximation and respiration sensor signals during respiration task. CCFA: Cumulative curve fitting approximation, fNIRS: Functional near-infrared spectroscopy

4. The BAR is defined as the ratio of half the range of the limits of agreement–representing the interval within which approximately 95% of the differences between two measurement methods are expected to fall–to the mean of the paired measurements. This relationship is expressed in Eq. 4:

$$BAR = \frac{1.96\ sd(x_1 - x_2)}{mean(\frac{x_1 + x_2}{2})} \quad x_1, x_2 : data\ of\ two\ methods \qquad (4)$$

These metrics serve as standardized measures to assess the agreement between HR measurements derived from the fNIRS or photo-plethysmography and the ECG signal.[17,18] The results indicate that the proposed algorithm demonstrates a strong Spearman linear correlation of 92.11 ± 0.81% between HRV extracted from fNIRS and ECG on the test dataset (unseen subjects). In addition, the BAR is below 6, signifying a good level of agreement [Table 1]. The results highlight the superiority of the CCFA method over the BPF approach in all evaluated criteria for HRV extraction. Specifically, the proposed method outperforms BPF due to its use of nonstationary filtering, which ensures that peak locations remain undistorted, a crucial factor for reliable HRV signal extraction and a significant advantage over traditional filtering techniques.

Result of applying respiratory rate estimation algorithm to *in vivo* measured functional near-infrared spectroscopy signal

Figure 8 illustrates an example of the raw optical fNIRS signal alongside its corresponding filtered signal using the CCFA method, with identified peaks. Additionally, the

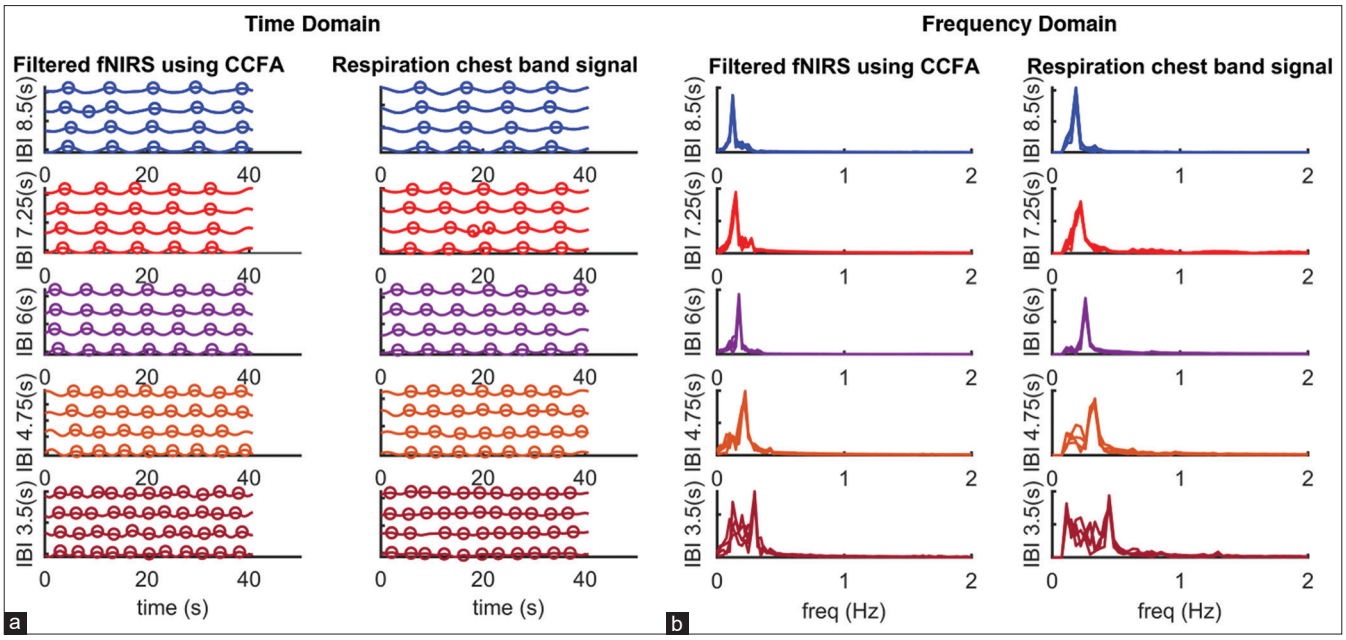

Figure 9: Time and frequency analysis of respiration signals from proposed method and chest band sensor. (a) Filtered functional near-infrared spectroscopy (fNIRS) signals (left) and corresponding respiration signals (right) for one subject, comprising four trials across five respiration duration speeds (inter beat interval = [3.5s …8.5s]). (b) Frequency domain representation of filtered fNIRS signals (left) and chest band signals (right). CCFA: Cumulative curve fitting approximation, fNIRS: Functional near-infrared spectroscopy

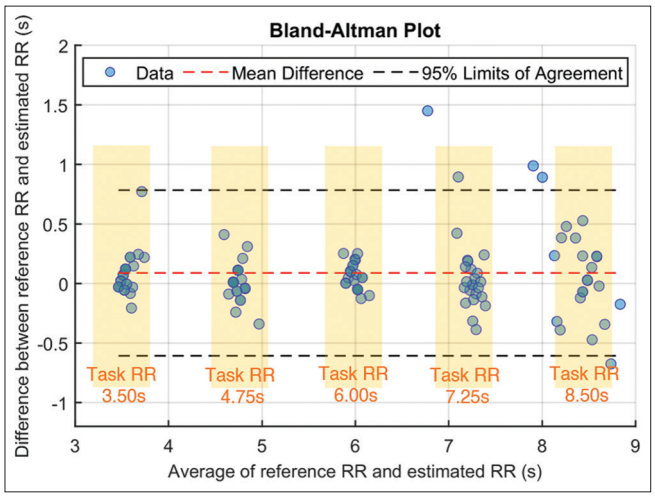

Figure 10: The Bland-Altman plot comparing the estimated respiration duration from functional near-infrared spectroscopy and the respiration sensor. The data are categorized into five highlighted areas representing respiration duration speeds (inter beat interval = [3.5s … 8.5s]) for all participants. RR: Respiratory rate

respiration signal from the strain gauge sensor, serving as a reference, is overlaid with its respective peaks from participant 1 during the respiration task. It is noteworthy that this is the first instance, to the best of our knowledge, where respiration (baseline-wander-related signal) is extracted directly from the optical signal rather than from HbO2 concentration, without utilizing the Modified Beer–Lambert Law.

The respiration task involves five respiration periods ranging from fast respiration with a period of 3.5 s to slower respiration with a period of 8.5 s, with intervals of 1.25 s. Each respiration period consists of four 50-s trials for each participant. Figure 9a depicts the filtered fNIRS signal using the proposed method, with its four trials displayed for each of the five respiration periods arranged from top to bottom on the left side of the figure. The first and last 5 s of each trial are excluded due to transitions between tasks. On the right side of the figure, corresponding signals from the respiration strain gauge sensor attached to the participant's body with a chest band are shown. In addition, peaks of each signal are calculated using our peak detection algorithm and are displayed in the figure.

Figure 9b illustrates the frequency energy using FFT for the participants. On the left, the frequency energy derived from the filtered fNIRS signal is shown, with each subplot containing four frequency spectra representing the four repetitions of the respiration task for a specific respiration rate. On the right, the corresponding frequency energy from the respiration sensor is displayed. For estimating respiration rate, one approach is to identify the peak of the FFT of the filtered signal, as utilized in a similar manner in Article.[21] However, we opted to employ our peak detection algorithm and calculate the adjacent peaks to determine the inter-breath interval (IBI). The median IBI obtained from this process was then utilized as the final estimation of the breath duration. The mean absolute error (AE) between the reference and estimated respiratory durations is provided for each subject is shown in Table 2. Considering that each subject in the respiration task completed 20 blocks of respiration, RR was estimated using both the proposed fNIRS-based method and the reference strain gauge. A paired *t*-test was conducted for each subject to compare

the two measurements, and no significant difference was observed across all subjects ($P > 0.05$). The average AE across all trials in test dataset is reported as 0.18s. In addition, to evaluate the overall performance of the proposed method, a Bland–Altman plot [Figure 10] was utilized. This method assesses the agreement between reference and estimated RRs by plotting the difference between each estimate and the references against their mean.

Discussion

This study aimed to investigate the feasibility of extracting HRV and respiration parameters from fNIRS signals using a novel filtration technique called CCFA. Concurrent recordings of fNIRS, ECG, and respiration with a chest band strain gauge were obtained from participants during a controlled respiration task. Real-time window-based peak detection algorithms were applied, and two-third of the dataset was used to optimize the parameters of the proposed method. By applying the peak location correction method based on polynomial fitting, as outlined in Algorithm 1, a significant improvement in HRV extraction was observed, with the correlation increasing from 81.32% to 92.11%. Although up-sampling the fNIRS data from 10 Hz to 100 Hz could be considered, the polynomial fitting approach, focused solely on the detected candidate peaks, proved more effective in enhancing performance. To assess the agreement between the physiological parameters derived from fNIRS signals and those obtained from ECG and respiration reference measures, correlation coefficients such as Pearson, Spearman, and intra-class were computed. In addition, the BAR was utilized to quantify the agreement between HRV from fNIRS and ECG. The results showed a high degree of agreement ($r > 0.92$, BAR <6%) between the extracted HRV and reference measures. Moreover, paired *t*-tests revealed no significant difference between the respiration periods estimated from fNIRS and the reference for all subjects, with mean AEs of 0.18 s for respiration period and 0.32 breaths per minute (bpm) for respiration rate. However, the study has several limitations that warrant consideration in future research. First, the use of CCFA with a large window size may not be suitable for real-time processing due to its time-consuming nature. Down-sampling the CCFA window could potentially enhance its efficiency. Second, the simplicity of the data recording protocol minimized contamination of fNIRS data by motion artifacts, necessitating further investigation into the performance of the peak detection algorithm with datasets containing more artifacts. Finally, the reliability of the proposed method was assessed only on young healthy subjects, highlighting the need to evaluate its robustness across diverse cohorts, including elderly individuals, neonates, and patients, as age-related factors may impact the performance of RR estimation algorithms.[34]

In comparing the results of this study with previous research, the current approach achieved a mean AE of 0.32 breath per minute in estimating RR, while the method reported in article[21] yielded a mean AE of 1.3 breath per minute. Another recent study focusing on neonates reported a mean AE of 1.1 breath per minute.[26] This study intentionally narrowed the range of the respiration period during the task from 2.5s to 10s[21] to 3.5s to 8.5s, influenced by the typical respiratory period for healthy adults at rest, which falls within the range from 3.5s to 5s or approximately 12–18 breaths per minute. By focusing on a narrower range closer to this typical respiratory

Table 1: Comparison of the heart rate variability derivation algorithm from functional near-infrared spectroscopy with reference electrocardiogram on the training dataset using five-fold cross-validation, along with the test dataset made up of completely unseen subjects

Subjet/fold	BPF				CCFA method			
	Mean error (s)	Maximum error (s)	Correlation (%)	BAR (%)	Mean error (s)	Maximum error (s)	Correlation (%)	BAR (%)
Train data								
Fold 1	0.053	0.142	91.37	6.48	0.014	0.093	94.25	5.87
Fold 2	0.036	0.137	90.17	6.21	0.012	0.098	92.33	5.24
Fold 3	0.061	0.172	91.53	6.87	0.018	0.124	91.27	6.02
Fold 4	0.059	0.128	92.12	6.12	0.013	0.126	94.51	5.39
Fold 5	0.044	0.153	90.89	6.39	0.012	0.137	93.46	5.32
Average	0.051	0.146	91.22	6.41	0.014	0.116	93.16	5.57
Test data								
Subject 1	0.061	0.157	90.91	6.22	0.013	0.112	93.15	5.27
Subject 2	0.055	0.149	91.17	5.79	0.015	0.140	92.81	6.00
Subject 3	0.062	0.161	89.98	6.32	0.016	0.142	91.13	6.02
Subject 4	0.059	0.173	90.31	6.45	0.016	0.134	92.21	5.92
Subject 5	0.063	0.167	90.42	6.71	0.017	0.128	91.24	5.72
Average	0.060	0.161	90.56	6.30	0.015	0.131	92.11	5.78

BPF – Bandpass filtering; CCFA – Cumulative curve fitting approximation; BAR – Bland-Altman Ratio

period, the experimental conditions were aligned more closely with physiological norms. However, this deliberate narrowing of the respiration period range does pose a limitation to the generalizability of the findings, as the algorithm's performance was primarily tested on seated adults in a resting state. This limitation implies that the algorithm's effectiveness may vary when applied to individuals in different conditions or populations, such as those engaged in physical activity[35] or individuals with respiratory conditions, as well as across various age groups.[36-38] In addition, differences in task design between the referenced studies may account for variations in results. Future studies should address these limitations to advance the applicability and reliability of fNIRS-based physiological monitoring techniques. Nevertheless, the findings indicate that the CCFA method can be among the top approaches for estimating RR, extracting HRV, and determining HR from fNIRS data.

Conclusions

In this study, novel algorithms were developed for extracting respiration and HRV from fNIRS signals without assuming quasi periodicity or stationarity. All filtering processes were conducted using the nonstationary processing method called CCFA. By employing a single fNIRS device, both brain activity and physiological parameters such as HR and respiration could be accurately extracted. Notably, only the optical signal was utilized without considering the concentration of the fNIRS signal, such as HbO2. The proposed method offers a versatile approach for approximating RR, HR, and HRV in applications where the analysis of both cerebral and physiological activities may synergize.

Table 2: The average absolute error between respiration duration extracted from reference and filtered functional near-infrared spectroscopy

Subjet/ fold	Respiration duration in task				
	8.50 s	7.25 s	6.00 s	4.75 s	3.50 s
Train data					
Fold 1	0.29	0.36	0.17	0.09	0.10
Fold 2	0.23	0.42	0.14	0.14	0.12
Fold 3	0.31	0.11	0.13	0.14	0.11
Fold 4	0.29	0.35	0.08	0.12	0.13
Fold 5	0.25	0.18	0.13	0.14	0.13
Average	0.27	0.28	0.10	0.13	0.12
Test data					
Subject 1	0.31	0.12	0.15	0.11	0.13
Subject 2	0.23	0.35	0.11	0.14	0.15
Subject 3	0.27	0.17	0.14	0.12	0.14
Subject 4	0.30	0.37	0.09	0.14	0.09
Subject 5	0.29	0.28	0.13	0.16	0.11
Average	0.28	0.26	0.12	0.13	0.12

Acknowledgments

The authors would like to thank all of the people who participated in the study, including subjects and students who collaborated.

Financial support and sponsorship

Nil.

Conflicts of interest

There are no conflicts of interest.

References

1. Fantini S, Frederick B, Sassaroli A. Perspective: Prospects of non-invasive sensing of the human brain with diffuse optical imaging. APL Photonics 2018;3:110901.
2. Mesquita RC, Franceschini MA, Boas DA. Resting state functional connectivity of the whole head with near-infrared spectroscopy. Biomed Opt Express 2010;1:324-36.
3. White BR, Snyder AZ, Cohen AL, Petersen SE, Raichle ME, Schlaggar BL, *et al.* Resting-state functional connectivity in the human brain revealed with diffuse optical tomography. Neuroimage 2009;47:148-56.
4. Shali RK, Setarehdan SK, Seifi B. Functional near-infrared spectroscopy based blood pressure variations and hemodynamic activity of brain monitoring following postural changes: A systematic review. Physiol Behav 2024;281:114574.
5. Sassaroli A, Pifferi A, Contini D, Torricelli A, Spinelli L, Wabnitz H, *et al.* Forward solvers for photon migration in the presence of highly and totally absorbing objects embedded inside diffusive media. J Opt Soc Am A Opt Image Sci Vis 2014;31:460-9.
6. Almajidy RK, Mankodiya K, Abtahi M, Hofmann UG. A newcomer's guide to functional near infrared spectroscopy experiments. IEEE Rev Biomed Eng 2020;13:292-308.
7. Chao J, Zheng S, Wu H, Wang D, Zhang X, Peng H, *et al.* fNIRS evidence for distinguishing patients with major depression and healthy controls. IEEE Trans Neural Syst Rehabil Eng 2021;29:2211-21.
8. Luke R, Shader MJ, McAlpine D. Characterization of Mayer-wave oscillations in functional near-infrared spectroscopy using a physiologically informed model of the neural power spectra. Neurophotonics 2021;8:041001.
9. Gao Y, Chao H, Cavuoto L, Yan P, Kruger U, Norfleet JE, *et al.* Deep learning-based motion artifact removal in functional near-infrared spectroscopy. Neurophotonics 2022;9:041406.
10. Shirvan RA, Setarehdan SK, Nasrabadi AM. A new approach to estimating the evoked hemodynamic response applied to dual channel functional near infrared spectroscopy. Comput Biol Med 2017;84:9-19.
11. Izzetoglu M, Bunce SC, Izzetoglu K, Onaral B, Pourrezaei K. Functional brain imaging using near-infrared technology. IEEE Eng Med Biol Mag 2007;26:38-46.
12. Nguyen HD, Yoo SH, Bhutta MR, Hong KS. Adaptive filtering of physiological noises in fNIRS data. Biomed Eng Online 2018;17:180.
13. Ortega-Martinez A, Von Lühmann A, Farzam P, Rogers D, Mugler EM, Boas DA, *et al.* Multivariate Kalman filter regression of confounding physiological signals for real-time classification of fNIRS data. Neurophotonics 2022;9:025003.
14. Bauernfeind G, Wriessnegger SC, Daly I, Müller-Putz GR. Separating heart and brain: On the reduction of physiological

noise from multichannel functional near-infrared spectroscopy (fNIRS) signals. J Neural Eng 2014;11:056010.
15. Eastmond C, Subedi A, De S, Intes X. Deep learning in fNIRS: A review. Neurophotonics 2022;9:041411.
16. Rajendra Acharya U, Paul Joseph K, Kannathal N, Lim CM, Suri JS. Heart rate variability: A review. Med Biol Eng Comput 2006;44:1031-51.
17. Schäfer A, Vagedes J. How accurate is pulse rate variability as an estimate of heart rate variability? A review on studies comparing photoplethysmographic technology with an electrocardiogram. Int J Cardiol 2013;166:15-29.
18. Hakimi N, Setarehdan SK. Stress assessment by means of heart rate derived from functional near-infrared spectroscopy. J Biomed Opt 2018;23:1-12.
19. Grassmann M, Vlemincx E, von Leupoldt A, Mittelstädt JM, Van den Bergh O. Respiratory changes in response to cognitive load: A systematic review. Neural Plast 2016;2016:8146809.
20. Wientjes CJ, Grossman P, Gaillard AW. Influence of drive and timing mechanisms on breathing pattern and ventilation during mental task performance. Biol Psychol 1998;49:53-70.
21. Hakimi N, Shahbakhti M, Sappia S, Horschig JM, Bronkhorst M, Floor-Westerdijk M, *et al.* Estimation of respiratory rate from functional near-infrared spectroscopy (fNIRS): A new perspective on respiratory interference. Biosensors (Basel) 2022;12:1170.
22. Patashov D, Menahem Y, Gurevitch G, Kameda Y, Goldstein D, Balberg M. fNIRS: Non-stationary preprocessing methods. Biomed Signal Process Control 2023;79:104110.
23. Pinti P, Scholkmann F, Hamilton A, Burgess P, Tachtsidis I. Current status and issues regarding pre-processing of fNIRS neuroimaging data: An investigation of diverse signal filtering methods within a general linear model framework. Front Hum Neurosci 2018;12:505.
24. Ye JC, Tak S, Jang KE, Jung J, Jang J. NIRS-SPM: Statistical parametric mapping for near-infrared spectroscopy. Neuroimage 2009;44:428-47.
25. Patashov D, Menahem Y, Ben-Haim O, Gazit E, Maidan I, Mirelman A, *et al.* Methods for gait analysis during obstacle avoidance task. Ann Biomed Eng 2020;48:634-43.
26. Hakimi N, Shahbakhti M, Horschig JM, Alderliesten T, Van Bel F, Colier WN, *et al.* Respiratory rate extraction from neonatal near-infrared spectroscopy signals. Sensors (Basel) 2023;23:4487.
27. Svinkunaite L, Horschig JM, Floor-Westerdijk MJ. Employing cardiac and respiratory features extracted from fNIRS signals for mental workload classification. In: Shadgan B, Gandjbakhche AH, editors. Biophotonics in Exercise Science, Sports Medicine, Health Monitoring Technologies, and Wearables II. Online Only, United States: SPIE; 2021. p. 13. Available from: https://www.spiedigitallibrary.org/conference-proceedings-of-spie/11638/2587155/Employing-cardiac-and-respiratory-features-extracted-from-fNIRS-signals-for/10.1117/12.2587155.short. [Last accessed on 2024 Oct 06].
28. Arefi Shirvan R, Setarehdan SK, Motie Nasrabadi A. Classification of mental stress levels by analyzing fNIRS signal using linear and non-linear features. Int Clin Neurosci J 2018;5:55-61.
29. Madhav KV, Ram MR, Krishna EH, Komalla NR, Reddy KA. Robust extraction of respiratory activity from PPG signals using modified MSPCA. IEEE Trans Instrum Meas 2013;62:1094-106.
30. Lee OW, Mao D, Savkovic B, Wunderlich J, Nicholls N, Jeffreys E, *et al.* The use of heart rate responses extracted from functional near-infrared spectroscopy data as a measure of speech discrimination ability in sleeping infants. Ear Hear 2023;44:776-86.
31. Pollonini L, Olds C, Abaya H, Bortfeld H, Beauchamp MS, Oghalai JS. Auditory cortex activation to natural speech and simulated cochlear implant speech measured with functional near-infrared spectroscopy. Hear Res 2014;309:84-93.
32. Trajkovic I, Scholkmann F, Wolf M. Estimating and validating the interbeat intervals of the heart using near-infrared spectroscopy on the human forehead. J Biomed Opt 2011;16:087002.
33. Perdue KL, Westerlund A, McCormick SA, Nelson CA 3rd. Extraction of heart rate from functional near-infrared spectroscopy in infants. J Biomed Opt 2014;19:067010.
34. Charlton PH, Bonnici T, Tarassenko L, Alastruey J, Clifton DA, Beale R, *et al.* Extraction of respiratory signals from the electrocardiogram and photoplethysmogram: Technical and physiological determinants. Physiol Meas 2017;38:669-90.
35. Blackie SP, Fairbarn MS, McElvaney NG, Wilcox PG, Morrison NJ, Pardy RL. Normal values and ranges for ventilation and breathing pattern at maximal exercise. Chest 1991;100:136-42.
36. Rodríguez-Molinero A, Narvaiza L, Ruiz J, Gálvez-Barrón C. Normal respiratory rate and peripheral blood oxygen saturation in the elderly population. J Am Geriatr Soc 2013;61:2238-40.
37. Tveiten L, Diep LM, Halvorsen T, Markestad T. Respiratory rate during the first 24 hours of life in healthy term infants. Pediatrics 2016;137:e20152326.
38. Fleming S, Thompson M, Stevens R, Heneghan C, Plüddemann A, Maconochie I, *et al.* Normal ranges of heart rate and respiratory rate in children from birth to 18 years of age: A systematic review of observational studies. Lancet 2011;377:1011-8.